especially $\Delta G^{\ddagger}$ for the former case are much smaller than those for Cs^+·C221. This could be a result of the larger stability of Cs^+·C221 cryptate due to the "cryptate effect". On the other hand, the $\Delta S^{\ddagger}$ value for the Cs^+·C22 complex is more positive than that for the Cs^+·C221 cryptate. We can reasonably assume that this variance is due to the difference between the exchange mechanisms of the cesium ion between the solvated and the complexed sites.

Acknowledgment. We gratefully acknowledge the support of this work by the National Science Foundation, Grant No. CHE-8515474.

Registry No. C222, 23978-55-4; C221, 31250-06-3; Cs^+, 18459-37-5.

The F + HN_3 System: A Chemical Source for NF($a^1\Delta$)

J. Habdas,† S. Wategaonkar, and D. W. Setser*

Department of Chemistry, Kansas State University, Manhattan, Kansas 66506 *(Received: August 8, 1986)*

The secondary reaction in the F + HN_3 reaction system under conditions of excess [F] provides a good source of NF($a^1\Delta$) in a flow reactor. Comparison of the NF(a) yield from the F/HN_3 system with the yield from the H/NF_2 system suggests that ≳85% of the HN_3 can be converted to NF(a). The F + N_3 secondary reaction has a rate constant of $(5 \pm 2) \times 10^{-11}$ cm^3 $molecule^{-1}$ s^{-1}. The primary reaction yields HF(v) with a distribution, P_1–P_4, of 36:36:22:06; the HF($v \geq 1$) formation rate constant is $(8.5 \pm 0.9) \times 10^{-11}$ cm^3 $molecule^{-1}$ s^{-1}. From the highest observed HF(v,J) level, D_0(H–N_3) and $\Delta H_f°_0$ (N_3) were assigned as ≤93 and ≤113 kcal mol^{-1}, respectively. Qualitative observations suggest a bimolecular NF(a) self-removal rate constant or a HF quenching rate constant of $\sim 5 \times 10^{-13}$ cm^3 $molecule^{-1}$ s^{-1}.

Introduction

The F atom + hydrazoic acid gas-phase reaction system has been studied by the fast-flow reactor technique. The primary reaction, formation of HF and N_3, and the secondary reaction between F and N_3 have been elucidated by monitoring the emission from the HF(Δv=1) and NF($a^1\Delta$–$X^3\Sigma^-$) transitions. The primary step has been previously studied by the arrested relaxation method[1] and the secondary steps have been qualitatively investigated[2-5] in flow reactors. Our results provide refinement to the prior studies. There are only a few ways to chemically produce the NF($a^1\Delta$ and $b^1\Sigma^+$) metastable states. One of the more successful for NF(a) is the H + NF_2 reaction.[6,7] Since N_2F_4, the simplest precursor to NF_2, is not readily available, discharges in NF_3 also have been used.[5] We have found that F + HN_3 system with excess [F] to be a convenient laboratory method for production of NF(a) radicals. Providing that F atoms can be tolerated, the F + HN_3 system has fewer kinetic complications than H + NF_2, since H atoms react with NF(a) to give N atoms.[7]

The primary reaction between F and HN_3 has been discussed in terms of three mechanisms.[1,2]

$$F + HN_3 \rightarrow HF + N_3 \quad (1)$$

$$F + HN_3 \rightarrow [HFN_3]^* \rightarrow HF + N_3 \quad (2)$$

$$F + HN_3 \rightarrow N_2 + [HNF]^* \rightarrow HF + N \quad (3)$$

The experiments to be presented here in which HF(v=1–4) were observed by infrared chemiluminescence are not consistent with formation of HF(v) in a secondary reaction involving F atoms, and HF(v) formation via reaction of F with HNF can be discounted.[1b] Since reaction 3 offers no possibility for a secondary reaction giving NF(a), and since the present study shows that NF(a) formation is a major aspect of the F/HN_3 system, reaction 3 also can be discarded as a *major* primary step. A less direct argument is that *under our conditions* there was no evidence for the presence of N atoms. Therefore, either direct H abstraction or addition of F followed by HF elimination from HFN_3* seems to be the only possibilities for the major primary reaction. Based upon the HF(v) distribution observed here, the direct abstraction mechanism probably is the more important.

In addition to studying the primary reaction from the HF(Δv=1) infrared chemiluminescence, the NF(a–X) emission intensity was used to assign a rate constant for the formation of NF($a^1\Delta$).

$$F(^2P) + N_3(X^2\Pi_g) \rightarrow NF(a^1\Delta) + N_2 \quad \Delta H°_0 = -40 \text{ kcal mol}^{-1} \quad (4a)$$

$$\rightarrow NF(X^3\Sigma^-) + N_2 \quad \Delta H°_0 = -72 \text{ kcal mol}^{-1} \quad (4b)$$

$$\rightarrow NF(b^1\Sigma^+) + N_2 \quad \Delta H°_0 = -18 \text{ kcal mol}^{-1} \quad (4c)$$

The $\Delta H°_0$ values are based on the $\Delta H_f°_0(N_3)$ determined in this work. Comparison of the NF(a) concentration from (4) with that from H + NF_2 for a known [NF_2] shows that HN_3 can be converted to NF(a) with high efficiency. The minor yield of NF(b) observed in the F/HN_3 system is consistent with formation from vibrational-to-electronic energy transfer between HF(v) and NF(a), although a very small direct formation component from (4c) is possible. The F/HN_3 system was investigated over a NF(a) concentration range of $(0.3–7) \times 10^{12}$ molecules cm^{-3}; the experiments at the higher concentrations provide estimates for the bimolecular self-destruction rate constants for N_3 and for NF(a). In subsequent work to be published from this laboratory, we will use the F/HN_3 system as an NF(a) source to measure the vibrational-to-electronic energy-transfer rate constants for HF(v) reacting with NF(a) to give NF(b).[9]

Experimental Techniques

Experiments were done in either of two tubular-flow reactors differing mainly in tube diameter and hence flow velocity; both reactors used the same pumping station, a Roots blower (M.D Pneumatics Inc., 4300 L/min) backed up by a mechanical pump (Sargent-Welch, 1500 L/min). The fast-flow reactor for ob-

† Permanent address: Institute of Chemistry, Silesian University, 40-006 Katowice, Poland.

(1) (a) Sloan, J. J.; Watson, D. G.; Wright, J. S. *Chem. Phys.* **1979**, *43*, 1. (b) Sloan, J. J.; Watson, D. G.; Wright, J. S. *Chem. Phys.* **1981**, *63*, 283.
(2) (a) Coombe, R. D.; Pritt, Jr., A. T. *Chem. Phys. Lett.* **1978**, *58*, 606. (b) Pritt, Jr., A. T.; Coombe, R. D. *Int. J. Chem. Kinet.* **1980**, *12*, 741. (c) Pritt, Jr., A. T.; Patel, D.; Coombe, R. D. *Int. J. Chem. Kinet.* **1984**, *16*, 977.
(3) Clyne, M. A. A.; White, I. F. *Chem. Phys. Lett.* **1970**, *6*, 465.
(4) Macdonald, R. G.; Sloan, J. J. *Chem Phys. Lett.* **1979**, *61*, 137.
(5) Herbelin, J. M.; Cohen, N. *Chem. Phys. Lett.* **1973**, *20*, 605.
(6) Malins, R. J.; Setser, D. W. *J. Phys. Chem.* **1981**, *85*, 1392.
(7) (a) Cheah, C. T.; Clyne, M. A. A.; Whitefield, P. D. *J. Chem. Soc., Faraday Trans. 2* **1980**, *76*, 711. (b) Cheah, C. T.; Clyne, M. A. A. *J. Chem. Soc., Faraday Trans. 2* **1980**, *6*, 1543. (c) Cheah, C. T.; Clyne, M. A. A. *J. Photochem.* **1981**, *15*, 21.
(8) (a) Agrawalla, B. S.; Setser, D. W. *J. Phys. Chem.* **1986**, *90*, 2450. (b) Manocha, A. S.; Setser, D. W.; Wickramaaratchi, M. A. *Chem. Phys.* **1983**, *76*, 129. (c) Agrawalla, B. S.; Setser, D. W. In *Gas Phase Chemiluminescence and Chemi-ionization*, Fontijn, A., Ed.; Elsevier: New York, 1985.
(9) Habdas, J.; Setser, D. W. *J. Phys. Chem.*, to be submitted.

0022-3654/87/2091-0451$01.50/0

servation of the HF(Δv=1) chemiluminescence was a 4-cm-diameter Pyrex tube in which the flow velocity was 120 m s^{-1}. The fluorine atoms and the argon carrier gas were added at the entrance to the reactor; the NaCl window for observation of the infrared emission was located 15 cm downstream. The F atoms entered from a centrally located 1.0-cm-diameter tube; the Ar flow was admitted through a circular loop with holes on the inner side to achieve uniform flow. A inlet located just in front of the NaCl observation window was used to introduce HN_3 to the fast-flow reactor. The distance between the reagent inlet and the center of the observation window was 2 cm, corresponding to a reaction time of ~0.15 ms with a total pressure of 0.7 Torr. A more detailed description of the fast-flow reactor used for infrared chemiluminescence studies can be found in other publications.[8]

The flow reactor used for the simultaneous observation of the HF(3–0), NF(a–X), and NF(b–X) emission was made from an 8-cm-diameter Pyrex glass tube of 86 cm length. This reactor was coated with halocarbon wax to reduce loss of F atoms to the walls and to protect the flow reactor from etching by fluorine and HF. However, a few experiments were done in an uncoated Pyrex glass reactor. All gas flows (except for the C_2H_6 used to monitor [F]) were introduced at the entrance to the 8-cm-diameter reactor. The total residence time with the Roots blower in operation was 40 ms for a pressure of 0.5 Torr. The reaction time increased to ~180 ms if the Roots blower was not used. Since the emissions to be measured were in the 500–850-nm range, they could be measured through the coated Pyrex walls of the reactor. The halocarbon coating plus the Pyrex wall did not affect the relative or total emission intensities, since these intensities were the same when compared through a quartz window located at the end of the reactor.

The F atoms were generated by the microwave discharge (60–70 W at 2.45 GHz) in a 17% CF_4/Ar mixture that was passed through a 10-mm-diameter alumina tube. The alumina tube was placed at the entrance of the flow reactor by insertion through an aluminum flange. The seal between this flange and the alumina and/or Pyrex tubes was made by epoxy cement. The F atom concentration in the 8-cm-diameter reactor, as measured by titration reactions, was approximately two times the CF_4 concentration when the Roots blower was operating, which suggests that most of the CF_4 was dissociated to CF_2 + 2F. For slower flow speeds the [F] was approximately equal to the [CF_4] metered to the reactor. The H atoms were generated in the same gas handling system as just described for F atoms by a microwave discharge in a flowing H_2/Ar mixture.

The Ar was taken from commercial cylinders and purified by passage through three molecular sieve filled traps at 196 K and 1 atm pressure. After each experiment the molecular sieve traps were reconditioned by heating to ~400 K at $\leq 10^{-3}$ Torr. The Ar flow rate was regulated by a needle valve and measured by a Fischer-Porter flow meter; the meter was calibrated by monitoring the pressure rise in a 12-L flask and by a wet test meter. The CF_4 (Matheson) and N_2F_4 (Aerospace Corp.) were purified by condensing samples, pumping on the frozen sample for several minutes, and subsequently loading a portion into a 12-L storage flask. The samples were diluted with dry argon to obtain mixtures of ~17% reagent concentration. The flow rates for all reagents were measured by recording the pressure rise in a calibrated volume. Hydrazoic acid was prepared from the reaction of NaN_3 and stearic acid;[10] 6.5 mmol of NaN_3 and a slight excess (6.7 mmol) of $C_{17}H_{35}COOH$ (both Aldrich Chemicals) were placed in a 250-mL flask containing a magnetic stirring bar. The flask with reagents was connected to a vacuum line and evacuated overnight. Then the flask was placed in a oil bath and heated to 380 K; the reagents form a liquid which was mixed with a magnetic stirrer. The gaseous HN_3 was collected in a 12-L flask, which was enclosed in a metal screen cage for safety. When the HN_3 pressure reached 50 Torr (~6 h), the heating was stopped and the sample was diluted with dry Ar to 300 Torr. This flask then was connected to the reagent line of the flow reactor from which the Ar/HN_3 mixture could be metered to the reactor. The above method provided a convenient source of water-free, gaseous HN_3. The N_2F_4 was placed in a storage vessel and passed through the same glass line as used for HN_3. The N_2F_4 was thermally dissociated by heating that portion (~1 m) of the 5-mm Pyrex line connecting the needle valve to the flow reactor to 200 °C. After the experiments there was no evidence for any etching of the glass line.

A 0.5-m monochromator (Minuteman) with 500-nm blazed grating and a cooled RCA-C131034 photomultiplier tube was used for observing the NF($b^1\Sigma^+$–$X^3\Sigma^-$) and NF($a^1\Delta$–$X^3\Sigma^-$) transitions at 529 and 874.5 nm, respectively, as well as the HF(3–0) emission at 860–890 nm. The monochromator was placed on a table that could be moved along the reactor, so that observation could be made for various reaction times. The response of the PM tube and monochromator was calibrated against a standard quartz–iodine lamp. This calibration in the range of 840 to 860 nm was confirmed by measuring the HF(3–0) emission lines for a Boltzmann rotational distribution. The HF(Δv=1) infrared chemiluminescence spectra from the F + HN_3 reaction was recorded with 2-cm^{-1} resolution with a Fourier-transform spectrometer (Digilab FTS-20) with a liquid-nitrogen-cooled InSb detector. The optical path and the space between the spectrometer and the flow path was purged with dry air to remove water vapor, which has a strong absorption for some of the low J lines of the HF(1–0) and HF(2–1) transitions. The wavelength response of the FT-IR spectrometer was calibrated with a blackbody source.

The relative concentrations of NF(a,v'=0), NF(b,v'=0), and HF(v=3) were determined from the integrated band areas of each emission system and the Einstein coefficients, which are 50, 0.18, and 1.6 s^{-1} for NF(b),[11] NF(a),[6] and HF(3–0),[12] respectively, and the response function of the monochromator. The actual measurements for [HF(3)] were based upon the band areas of several rotational lines of the HF(3–0) transition. The relative concentrations of the three species established from observations with the monochromator were placed upon an absolute basis by relating the NF(a–X) emission intensity to the [HN_3], vide infra. Although this was not done in the present work, these relative concentration measurements can be extended to HF(v=1 and 2) by observing simultaneously the HF(Δv=1) emissions with the FT-IR spectrometer and relating [HF(v=3)] to [HF(v=1 and 2)].[9] The requisite HF Einstein coefficients are available.[12]

Experimental Results

Determination of F-Atom Concentration. The concentration of F atoms in the 8-cm-diameter reactor was determined from two titration reactions[13–15]

$$H_2 + F \rightarrow HF + H \qquad k = 2.6 \times 10^{-11}\ cm^3\ molecule^{-1}\ s^{-1} \tag{5a}$$

$$Cl_2 + F \rightarrow ClF + Cl \qquad k = 1.6 \times 10^{-10}\ cm^3\ molecule^{-1}\ s^{-1} \tag{5b}$$

The relative [F] was monitored at the exit end of the flow reactor by the HF(3–0) emission intensity from the F + C_2H_6 reaction.[8] The C_2H_6 inlet was placed 90-cm downstream of the position where H_2 or Cl_2 was added to the reactor to give 40 ms of reaction time for the titration reactions. Addition of the H_2 or Cl_2 via the inlet normally used for HN_3 caused consumption of F atoms, as was evident from reduction of the HF(3–0) emission intensity. The HF(3–0) intensity decreased linearly for a sufficiently large range of [H_2] or [Cl_2] that extrapolations could be made to

(10) Krakow, B.; Lord, R. C.; Neely, G. O. *J. Mol. Spectrosc.* **1968**, *27*, 198.

(11) (a) Lin, D.; Setser, D. W. *J. Phys. Chem.* **1985**, *89*, 1561. (b) Tennyson, D. H.; Fontijn, A.; Clyne, M. A. A. *Chem. Phys.* **1981**, *62*, 171. (c) Cha, H.; Setser, D. W. *J. Phys. Chem.*, to be submitted.

(12) Oba, D.; Agrawalla, B. S.; Setser, D. W. *J. Quant. Spectrosc. Radiat. Transfer* **1985**, *34*, 283.

(13) Clyne, M. A. A.; Hodgson, A. *J. Chem. Soc., Faraday Trans. 2* **1985**, *81*, 443.

(14) Beman, P. P.; Clyne, M. A. A. *J. Chem. Soc., Faraday Trans. 2* **1976**, *72*, 191.

(15) Appelman, H. E.; Clyne, M. A. A. *J. Chem. Soc., Faraday Trans. 1* **1975**, *71*, 2072.

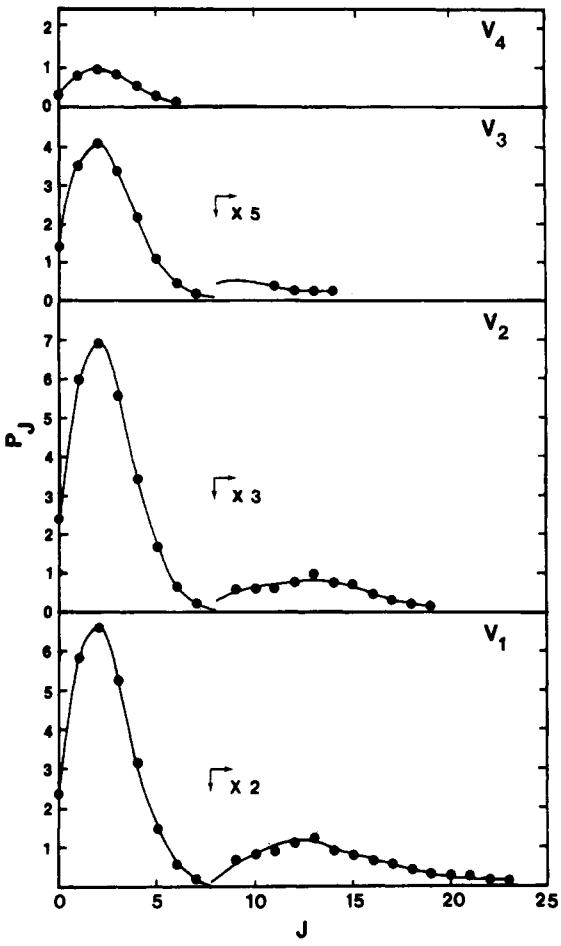

Figure 1. The HF(v,J) distributions from F + HN_3 observed after 0.15-ms reaction time in the fast-flow reactor at 0.7 Torr with $[HN_3]$ = 1.7 × 10^{12} molecules cm^{-3} and $[CF_4]$ = 1.14 × 10^{12} molecules cm^{-3}. P_1–P_4 = 37:37:21:05. Note the scaling factors used for plotting the high J envelopes of v = 1–3.

estimate the end point. In general, the [F] was slightly more than twofold larger than the $[CF_4]$ with the blower in operation for $[CF_4] \leq 5 \times 10^{12}$ molecules cm^{-3}, i.e., each CF_4 was dissociated to give 2 F atoms. If the flow speed was reduced by turning off the blower and if the $[CF_4]$ was increased to $\sim 7.5 \times 10^{12}$ molecules cm^{-3}, the [F] was approximately equal to $[CF_4]$. Some experiments with the blower in operation also were done with SF_6/Ar mixtures as the source of F atoms. The titration measurements for $[SF_6] \approx 2.5 \times 10^{12}$ molecules cm^{-3} gave approximately the same result as for the CF_4/Ar mixtures, i.e., 2 F atoms were formed per SF_6 molecule.

The Primary Reaction: HF(v) Formation Rate Constants. The HF(v) emission spectra were collected in the smaller diameter reactor as a function of both $[HN_3]$ and $[CF_4]$ for an observation time of ~0.15 ms. Figure 1 shows the rotational distribution for each HF(v) level at 0.7 Torr. These distributions consist of two envelopes: the relaxed Boltzmann (300 K) populated levels for $J \leq 7$ and a second envelope extending from $J \geq 9$. The envelope of high rotational levels is the residue of the nascent rotational distribution from the reaction. The steady-state fraction with $J \geq 9$ were 0.14, 0.062, and 0.009 for v = 1, 2, and 3, respectively. In order to obtain the nascent vibrational HF(v) distribution, data should be collected for conditions such that the steady-state distribution is independent of [F] and $[HN_3]$, i.e., the steady-state distribution is free of relaxation. For $[CF_4]$ or $[HN_3] \leq 2.5 \times 10^{12}$ molecules cm^{-3}, the observed HF(v) distribution was independent of the reagent concentration. This is demonstrated for $[HN_3]$ by the plot of the HF(v) distribution vs. $[HN_3]$ in Figure 2. A HF(v) distribution was assigned to the average P_v values for each plot vs. $[NH_3]$ for a given experiment. The results from several experiments are summarized in Table I; the three independent experiments are in good agreement and the statistical

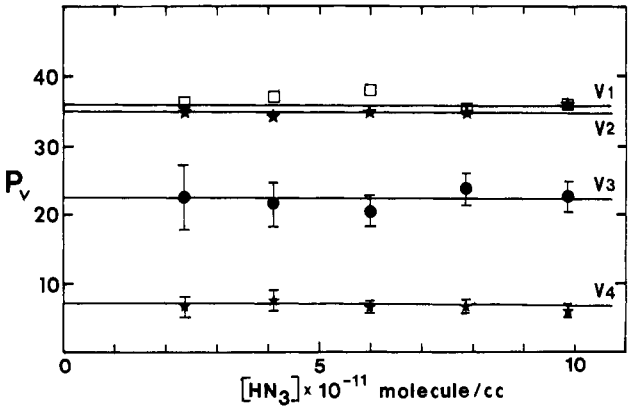

Figure 2. The dependence of the HF(v) distribution on $[HN_3]$ at constant $[CF_4]$ = 0.9 × 10^{12} molecule cm^{-3}. These data were obtained in the fast-flow reactor for 0.15-ms reaction time at 0.7 Torr. Error bars are shown only for the v = 3 and 4 data points; however, similar uncertainty holds for v = 1 and 2. The HF(v) distribution was independent of $[HN_3]$ for concentrations $\leq 2.5 \times 10^{12}$ molecules cm^{-3}.

TABLE I: HF Vibrational Distribution from the F + HN_3

expt no.	P_0	P_1	P_2	P_3	P_4	$\langle f_V \rangle^a$	comments
1		36	36	22	06		this work
2		35	37	22	06		this work
3		36	35	22	07		this work
		36[b]	36[b]	22[b]	06[b]		
	26[c]	26	26	17	05	0.37	
	15[c]	30	30	20	05	0.43	
		23[d]	19[d]	14[d]	06[d]		this work
		(42.0)	(42.5)	(43.4)	(45.5)		
		60	26	11	03		ref 1a
				16[d]	10[d]		ref 1a

[a] $\langle f_V \rangle = E_v/\langle E \rangle$; $\langle E \rangle = D_0(H\text{–}F) - D_0(H\text{–}N_3) + E_a + 3RT$ = 43.8 kcal/mol; since E_a was assumed to be ≈ 0 kcal/mol. [b] Average of the values from experiments 1 to 3; the uncertainty is ±10% for P_1–P_3 and ±20% for P_4. The $[CF_4]$ was 2.1, 1.1 and 0.91 molecules cm^{-3} for experiments 1–3. [c] P_0 was assigned by setting $P_0 = P_1$ and $P_0 = {}^1/_2P_1$. [d] The highest J levels observed for individual v levels (with corresponding E_V (kcal mol^{-1}) in parentheses).

uncertainty in the distribution is ±10%. The best estimate of the nascent HF(v) distribution is P_1–P_4 = 0.36:0.36:0.22:0.06. Explicit tests were made for HF(v=5), but the emission was *never* present. From the spectra with the best signal-to-noise ratio, the limit for [HF(v=5)] was less than 0.2% of [HF(v=1–4)].

The uncertainty in the P_v assignments arises mainly from the noise associated with the rotational lines. The analysis of each v level was performed by using all J lines in the 300 K Boltzmann envelope. The standard deviation in the HF(v) distribution deduced from the different rotational lines was typically 10% for v = 1–3 and about 20% for v = 4. The uncertainty did not change significantly with $[HN_3]$ except for the lowest concentration, 0.34 × 10^{12} molecule cm^{-3}, where it increased to 20% for all v levels. Boltzmann plots [log I_J/S_J vs. $J(J+1)$] were constructed for J = 0–5 of each v level. These plots were linear with temperatures of 300 ± 25 K and there was no systematic deviations associated with a given rotational level. Coaddition of repetitive scans by the FTIR spectrometer is sensitive to the fixed mirror alignment. Variations in the alignment during collection of a spectrum gives noise in the base line. This uncertainty is partially compensated by using several P and R lines to compute P_v. Water absorption in the 3900–3600-cm^{-1} region interferes with P branch of HF(1–0) and P and R branchs of HF(2–1). Although the lines ($1P_4$, $2R_4$, $2P_0$, $3R_4$) which are most strongly affected by water absorption were omitted from the analysis, other lines are affected weakly and this adds some additional uncertainty.

The estimate made for P_0 strongly influences the assignment of $\langle f_V(HF) \rangle$. If P_0 is assumed to be the same as P_1, $\langle f_V(HF) \rangle$ = 0.37. If P_0 is one-half of P_1, then $\langle f_V(HF) \rangle$ becomes = 0.43. The energy disposal for F + HN_3 is rather similar to that from F + H_2S, which proceeds by direct abstraction.[8] The available

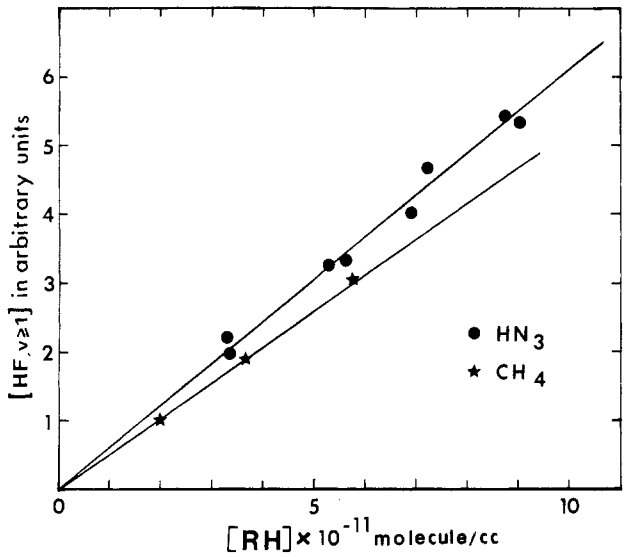

Figure 3. The relative HF($v \geq 1$) concentration (in arbitrary units) from F + HN_3 and F + CH_4 for identical Δt and [F] plotted against the respective reagent concentrations. The [CF_4] was 0.84 × 10^{12} molecule cm^{-3}.

energy is about 5 kcal mol^{-1} larger and the distribution is shifted somewhat in favor of higher v levels for H_2S with P_1–P_4 = 24:32:33:11 and $\langle f_V(HF) \rangle$ = 0.45.

The $D_0(H-N_3)$ was estimated from the highest J levels observed, see Table I, which were J = 19, 14, and 6 for v = 2, 3, and 4, respectively. The average energy limit from these observations gives $D_0(H-N_3)$ = 93.4 kcal mol^{-1} for an activation energy of zero. The v = 1 result (J_{max} = 23) was not included in the average because the spacing between J = 23 and J = 24 is so large (2.6 kcal mol^{-1}) that formation at J = 24 could be above the thermochemical limit. A value for $D_0(H-N_3)$ of 92 ± 5 kcal mol^{-1} has been reported from proton affinity measurement of azide ion,[16] which is about 12.5 kcal mol^{-1} larger than the previously accepted value of 79.4 kcal mol^{-1}. Except for reactions giving radicals with large stabilization energies, direct H atom abstraction reactions by F atoms generally yield HF(v,J) molecules in vibrational–rotational levels up to the energy limit permitted by the reaction[8] and the highest observed HF(v,J) levels give a reliable estimate of $D_0(H-N_3)$. Since our ≤93.4 kcal mol^{-1} value is close to the PA(N_3^-) measurement, a bond energy near 92–93 kcal mol^{-1} is favored for $H-N_3$. The previous infrared chemiluminescence study[1] reported very weak emission from HF(v=5) for high reagent flows, as well as the J_{max} values for HF(v=3 and 4) that are close to our values. The arrested relaxation data and their implications for the thermochemistry must be reevaluated and this will be done in the Discussion section.

Pairwise comparison were done with F + CH_4 and HN_3 under identical conditions to obtain the relative HF($v \geq 1$) formation rate constant. Since the rate constant for F + CH_4 (7.2 × 10^{-11} cm^3 $molecule^{-1}$ s^{-1}) is well-known,[17] comparison of the relative [HF($v \geq 1$)] from both reactions (Figure 4) yields the HF($v \geq 1$) formation rate constants for F + HN_3, which is (8.5 ± 0.9) × 10^{-11} cm^3 $molecule^{-1}$ s^{-1}. If P_0 is taken to equal P_1, the total HF(v) formation rate constant becomes (1.1 ± 0.1) × 10^{-10} cm^3 $molecule^{-1}$ s^{-1}. The HF(v) distribution from F + CH_4 was P_1–P_3 = 21:62:17, which agrees with prior work[8b] and shows that the flow reactor used in this work is satisfactory for obtaining nascent HF(v) distributions.

The Secondary Reaction: Formation of NF(a) in the 10^{12} molecule cm^{-3} Range. We will assume that N_3 is the main primary product and attribute the secondary steps to reaction 4. We observed the HF(v=3), NF(a), and NF(b) relative emission intensities for various reaction times by moving the monochromator

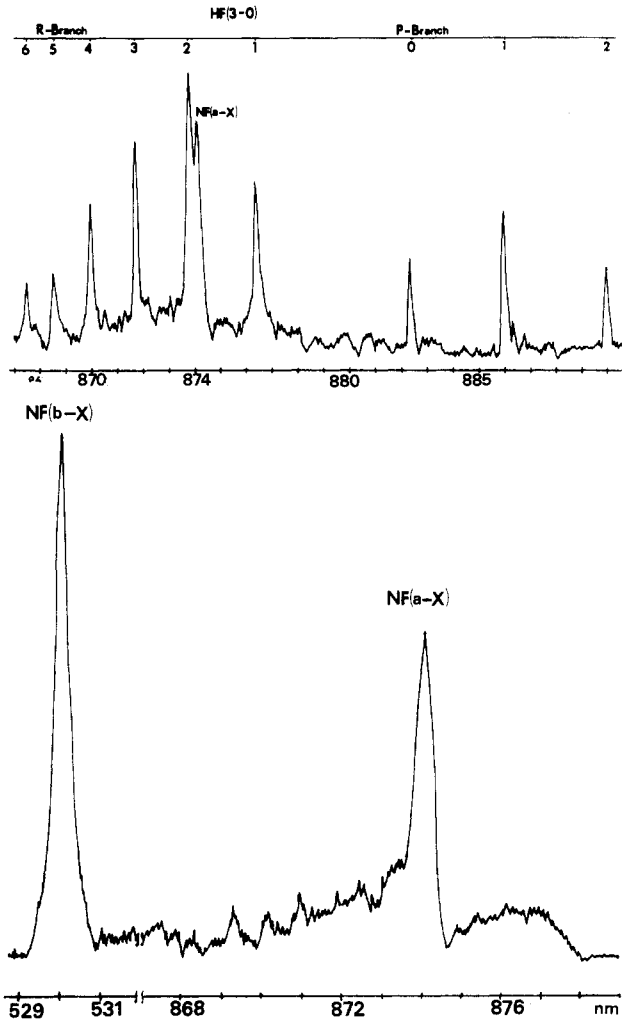

Figure 4. (a, top) The NF(a–X) and HF(3–0) emission spectra after 5-ms reaction time for [HN_3] = 1 × 10^{12} molecule cm^{-3} and [CF_4] = 3 × 10^{12} molecules cm^{-3}. (b, bottom) The NF(b–X) and NF(a–X) emission spectra after 50-ms reaction time for [HN_3] = 1 × 10^{12} molecule cm^{-3} and [CF_4] = 5 × 10^{12} molecules cm^{-3}. Note that the band envelope for NF(a–X) extends from 877 to 869 nm.

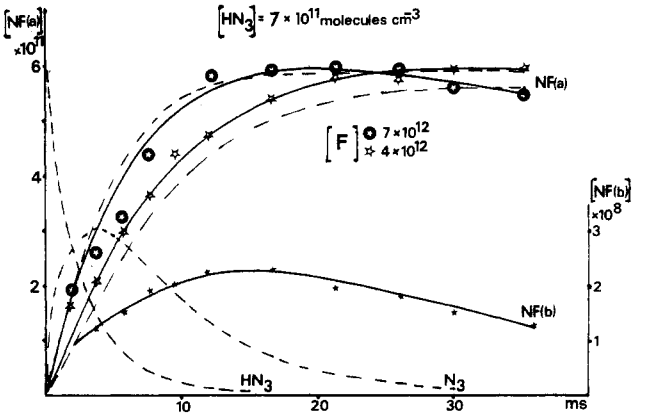

Figure 5. The NF(a) concentrations along the flow tube for two [F]; the NF(b) concentration is shown only for [F] = 4 × 10^{12} molecules cm^{-3}. The dotted curves show the [NF(a)], [HN_3], and [N_3] from numerical simulation of the rate equations for $k(F+N_3)$ = 5 × 10^{-12} cm^3 $molecule^{-1}$ s^{-1} and [F] = 4 × 10^{12} molecules cm^{-3}; the simulated [NF(a)] is also shown for the higher [F]. The [NF(a)] was scaled so that the maximum [NF(a)] is equal to 0.85[HN_3]; see text.

to different positions along the 8-cm-diameter flow tube. The NF(a–X) and HF(3–0) spectra were taken with sufficiently high resolution that the NF(a–X) band and the R2 line of HF(3–0) band could be deconvoluted, see Figure 4a. Despite repeated attempts, emission from the v' = 1 level of NF(a) or NF(b) was

(16) Pellerite, M. J.; Jackson, R. L.; Brauman, J. I. *J. Phys. Chem.* **1981**, *85*, 1624.
(17) Clyne, M. A. A.; Nip, W. S. *Int. J. Chem. Kinet.* **1978**, *10*, 383.

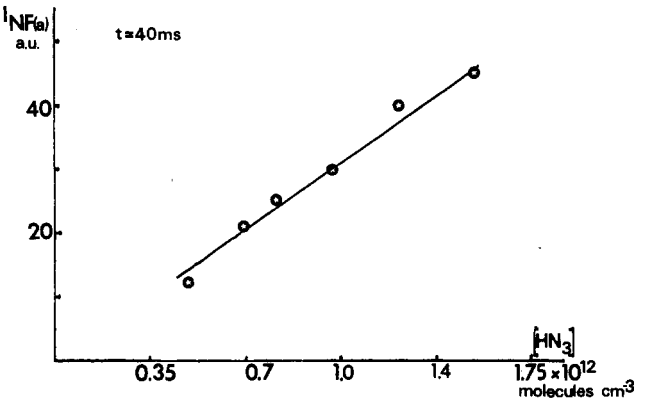

Figure 6. The dependence of the NF(a) emission intensity, arbitrary units, upon $[HN_3]$ for $[F] = 1 \times 10^{13}$ molecule cm^{-3}; the emission was observed after 40 ms of reaction time.

never observed, see Figure 4, and levels above $v' = 0$ need not be considered. Some typical [NF(a)] and [NF(b)] measurements for different [F] with $[HN_3] = 0.7 \times 10^{12}$ molecule cm^{-3} are shown in Figure 5. The relative NF(a) and NF(b) concentrations were assigned from the integrated band areas, the wavelength response function, and the Einstein coefficients. The quite different band shapes of the NF(a–X) and NF(b–X) transitions, see Figure 4b, *require* that band areas associated with the transitions be used to determine relative concentrations. The absolute NF(a) concentration in Figure 5 was assigned from equating the maximum [NF(a)] to $0.85[HN_3]$, vide infra. The NF(a) product definitely arises from a secondary reaction because there is a delay period before it can be observed, whereas HF(3–0) can be observed at a very early time. The rise time for [NF(a)] for various [F] suggests that the rate constant for reaction 4a is $(5 \pm 2) \times 10^{-11}$ cm^3 $molecule^{-1}$ s^{-1}, as will be discussed later.

For a given [F] and $[HN_3]$, the NF(b)/NF(a) ratio increases and then subsequently decreases with time. Although the ratio increased with [NF(a)] in the short time domain, the [NF(b)/NF(a)] ratio was always less than 10^{-4} in this work. The early time kinetics for NF(b) formation suggests that V–E transfer from collisions between HF($v \geq 2$) and NF(a) is an important formation step. Based upon some experiments with F + Cl–N_3, direct NF(b) formation cannot be entirely discounted. For the operating conditions of Figure 5, [NF(b)] reached a maximum at ~15 ms and thereafter declined. The decline is mainly a consequence of radiative decay, $\tau(NF(b)) \sim 20$ ms.[11] However, there is some quenching[11a] by HF(v=0), $k_Q = 9.7 \times 10^{-13}$ cm^3 $molecule^{-}$ s^{-1}, which has a concentration equal to the starting HN_3. The more rapid decay of [NF(b)] in the presence of higher [F] shown in Figure 5 implies that NF(b) also is quenched by F atoms or some other component from discharged CF_4, such as CF_2. The [HF(3)] formed in the primary step decays rapidly as a consequence of vibrational relaxation and radiative decay, and HF(v=3) cannot be observed after ≅10 ms, if [F] > $[HN_3]$. For [NF(a)] = [HF] ≤ 10^{12} molecule cm^{-3}, the quenching of NF(a) by HF to give HF(v=3) was too minor to be observed via HF(3–0) emission in the downstream part of the reactor.

A critical aspect about the F/HN_3 system as a NF(a) source is the yield of [NF(a)] relative to the starting $[HN_3]$. This was investigated in two ways. With excess F atoms, the [NF(a)] does increase linearly with $[HN_3]$ in the $(0.3–1.7) \times 10^{12}$ molecules cm^{-3} range, as shown in Figure 6 where [NF(a)] was observed after ~40 ms reaction time for $[F] \approx 1 \times 10^{13}$ molecule cm^{-3}. For fixed [F], the maximum [NF(a)] was found for $[HN_3] \lesssim {}^1/_2[F]$. Higher $[HN_3]$ caused a reduction in [NF(a)] because reaction 1 consumes the F atoms and prevents NF(a) formation from step 4. A more quantitative check upon the efficiency of NF(a) formation was made by comparing [NF(a)] from F + HN_3 to that from H + NF_2 for known $[NF_2]$ and excess [H]. Reaction 6 is known to be essentially stoichiometric.[6,7]

$$H + NF_2 \rightarrow HF + NF(a) \qquad k = (1.5 \pm 0.2) \times 10^{-11}\ cm^3\ molecule^{-1}\ s^{-1} \quad (6)$$

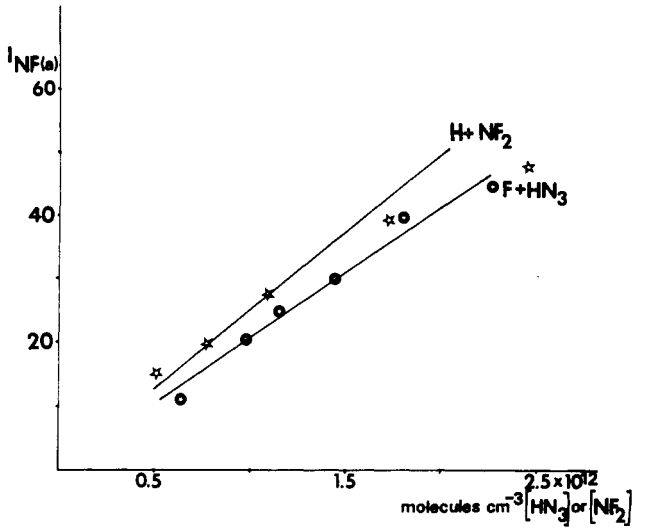

Figure 7. Comparison of the NF(a–X) emission intensity from the H + NF_2 and F + HN_3 reactions after 40 ms for excess [H] and excess [F], respectively. The last two points on the H + NF_2 plot were ignored in drawing the linear relationship.

A metered flow of N_2F_4 was passed through a heated (150 °C) glass lead line to provide NF_2, which was then reacted with excess H atoms. Comparisons were done in several experiments for ~10- and ~40-ms reaction times for both the F/HN_3 and H/NF_2 systems and some sample results are given in Figure 7. For equal flows of N_2F_4 and HN_3, the [NF(a)] from HN_3 was always $\lesssim {}^1/_2$ of that from N_2F_4. The results were quite reproducible and the average of four experiments, such as shown in Figure 7, gave $[NF(a)]_{HN_3} = (0.85 \pm 0.1)[NF(a)]_{NF_2}$ for excess [F] and [H], respectively. The $[HN_3]$ and $[NF_2]$ were less than $\leq 1.7 \times 10^{12}$ molecules cm^{-3} for these comparison experiments. Based upon the H + NF_2 comparison, we conclude that the [NF(a)] from reaction 4 was consistently ~0.85 of the $[HN_3]$ metered to the reaction vessel providing that $[F] \gtrsim 5[HN_3]$. Experiments with different HN_3 samples gave similar results, and there was no obvious dependence of the [NF(a)] yield on the given HN_3 preparation. Since the NF(b) concentration is insignificant, the remaining fraction of the $[HN_3]$ could correspond to NF(X) formation. However, other possibilities for the less than stoichiometric yield of [NF(a)] could be a contribution from reaction 3 and uncertainty in the $[NF_2]$ and $[HN_3]$ measurements. The bimolecular self-destruction of N_3 will become increasingly important at higher $[HN_3]$ and lower $[F]/[HN_3]$, but there is no indication that this loss mechanism affected the present NF(a) measurements.

A numerical simulation of the rate processes was done to establish the acceptable range for the F + N_3 rate constant and to check the mechanism for NF(b) formation. The model, Table II, included the primary and secondary reaction steps and the formation and various decay steps for NF(b) and HF(v). No provision was made for quenching of NF(a) except for V–E transfer with HF(v) and bimolecular self-destruction, which includes quenching by HF since [HF] = [NF(a)]. For the $[HN_3] = 1 \times 10^{12}$ molecule cm^{-3} range, [NF(a)] was constant after N_3 reacts with F and the NF(a) bimolecular self-destruction is not important. The self-destruction of N_3 was included, but for $[HN_3]$ less than 2×10^{12} molecules cm^{-3} and for $[F] > 4[HN_3]$ this process also is not important; further discussion is given in the following section. The destruction of N_3 on the wall was not included, but for certain experimental conditions this may be the dominant N_3 loss term. The assignment for k_4 is based upon the rise in [NF(a)] and independent of the imperfectly understood formation steps for NF(b) or the NF(a) decay at higher concentrations. As shown in Figure 5, an adequate fit was obtained for $k_4 = (5 \pm 2) \times 10^{-11}$ cm^3 $molecule^{-1}$ s^{-1}. The largest uncertainty in k_4 is associated with the [F], since the growth of [NF(a)] depends on $k_4[F]$. Further refinement in k_4 is not possible unless the [F] is measured with greater reliability. Our assignment

TABLE II: Kinetic Model for the F + HN_3 System[a]

reaction	rate constants[b]	literature
$F + HN_3 \rightarrow HF(0) + N_3$	2.9×10^{-11}	this work
$F + HN_3 \rightarrow NH(1) + N_3$	2.9×10^{-11}	this work
$F + HN_3 \rightarrow HF(2) + N_3$	3.0×10^{-11}	this work
$F + HN_3 \rightarrow HF(3) + N_3$	1.9×10^{-11}	this work
$F + HN_3 \rightarrow HF(4) + N_3$	4.4×10^{-12}	this work
$F + N_3 \rightarrow NF(a) + N_2$	5.0×10^{-11}	this work
NF(b) + F → NF(a or X) + F	1.0×10^{-13}	assumed[d]
NF(a) HF(v+2) → NF(b) + HF(v)	0.5×10^{-12}	c
NF(b) + HF(0) → NF(a) + HF(v+2)	1.0×10^{-12}	ref 9
$2N_3 \rightarrow 3N_2$	$\sim 2 \times 10^{-11}$	this work[e]
2NF(a) → 2NF(X) or N_2 + 2F	$\sim 6 \times 10^{-13}$	this work[e]
NF(b) → NF(X) + $h\nu$	50 s^{-1}	11
HF(3) → HF(2) + $h\nu$	411 s^{-1}	12
HF(2) → HF(1) + $h\nu$	325 s^{-1}	12
HF(1) → HF(0) + $h\nu$	190 s^{-1}	12

[a] The radiative decay of NF(a) was not included in the model because the lifetime is too long (5.6 s) for this process to be significant. [b] All rate constants are in cm^3 $molecule^{-1}$ s^{-1} units unless specified otherwise. [c] Assigned by detailed balance from NF(b) + HF(v). [d] Assigned to be consistent with the enhanced decay rate of NF(b) in presence of excess [F] and work in ref 11c. [e] Estimated, see text; the 2NF(a) process also could be quenching of NF(a) by HF.

is an order of magnitude larger than the previous estimate[2a] of k_4 ($\sim 2 \times 10^{-12}$ cm^3 $molecule^{-1}$ s^{-1}), which was made from similar observations but with much higher concentrations of F and HN_3 and in a teflon tubular reactor.

We also investigated the reaction of F atoms with ClN_3 as a source of NF(a). The ClN_3 was produced by passing Cl_2 over NaN_3 following the procedure recommended by Coombe.[18] Observations similar to those shown in Figures 5 and 6 were made for $[CF_4] = 1.0 \times 10^{13}$ and $[ClN_3] = 6.0 \times 10^{12}$ molecules cm^{-3}. The maximum ratio of NF(b) to NF(a) was $\sim 4 \times 10^{-4}$, which is slightly larger than in Figure 5. Obtaining a NF(a) concentration similar to that from a given $[HN_3]$ required 6–8 times higher $[ClN_3]$. Also the NF(a) concentration seemed to decay more rapidly than in the F/HN_3 system. Emission from NCl(b–X) was not observed, which suggests that the concentration of Cl atoms (from F + Cl_2) was sufficiently low that reaction of Cl with N_3 to give NCl(b) was not important and, hence, molecular Cl_2 must not have been a major contaminant in the Cl–N_3 sample. Assuming that our Cl–N_3 sample was reasonably pure, these data suggest that the primary reaction has two components

$$F + Cl\text{–}N_3 \rightarrow ClF + N_3 \quad (7a)$$

$$\rightarrow ClNF + N_2 \quad (7b)$$

and that [Cl–N_3] was not quantitatively converted to [N_3]. Since NF(b) was observed and since HF(v) should not have been present, this brief study suggests that F + N_3 may directly give some NF(b). Based upon these qualitative results and the extreme instability of ClN_3, the F/Cl–N_3 system is much less desirable than the F/HN_3 system as a NF(a) source.

The Secondary Reaction: Formation of NF(a) in the 10^{13} molecule cm^{-3} Range. Experiments were done for higher $[HN_3]$, variable excess [F], and reduced pumping speed to examine the NF(a) decay for higher concentrations and long times. Titration of the F atoms for these conditions showed that [F] = $[CF_4]$. Some characteristic results are shown in Figure 8; the [NF(a)] was assigned from the observed I[NF(a–X)] and the previously determined relation between the NF(a–X) intensity and absolute [NF(a)]. One important finding is that the maximum NF(a) emission intensity did scale as expected, with $[HN_3]$, providing that the [F] was in sufficiently large excess. For $[HN_3] \leq 4 \times 10^{12}$ molecules cm^{-3} and [F] = 3–4 times the $[HN_3]$, the long term decay of [NF(a)] was modest, i.e., the [NF(a)] declined to 0.8 of the maximum concentration after $\sim$0.2 s. However, as displayed in Figure 8, a definite decay of NF(a) develops as [NF(a)]

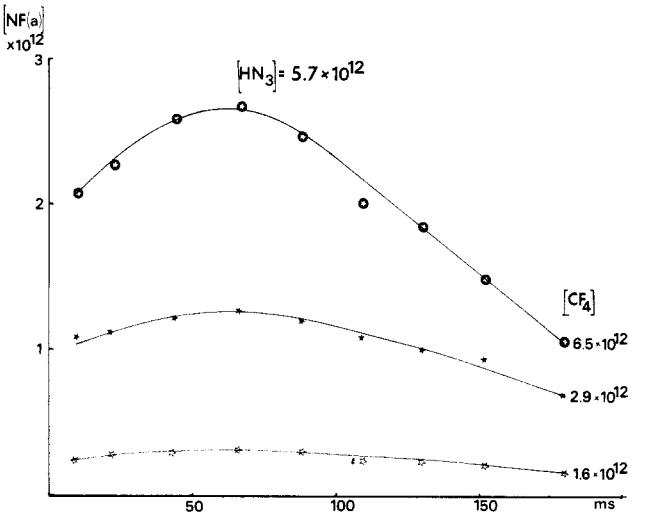

Figure 8. The time dependence of [NF(a)] for high concentration and long reaction time. The NF(a) concentration was assigned from the observed NF(a–X) emission intensity and the calibrated emission intensity for NF(a) = 0.7×10^{12} molecule cm^{-3} determined in Figure 5; the [F] are indicated in the figure. For the highest [F], the [NF(a)] should rise more quickly than shown in this figure, and, in fact, the majority of the experiments with large [F] did show the expected fast rise.

is increased further. This general behavior was observed in many independent experiments. This NF(a) decay can be associated with bimolecular self-destruction or with quenching by HF (or possibly some product from the CF_4 discharge).

$$NF(a) + NF(a) \rightarrow N_2 + 2F \text{ (or } 2NF(X)) \quad (8)$$

$$NF(a) + HF \rightarrow HF(v) + NF(X) \quad (9)$$

Since the NF(b–X) emission intensity does not go to a steady-state value and does not seem to depend upon [NF(a)], there is no evidence for an energy-pooling component to the NF(a) self-destruction reaction. Since [HF] is equal to [NF(a)], the kinetics for (8) and (9) are the same. If reaction 8 or 9 is assumed to be responsible for the NF(a) decay rate, we obtained $\sim 6 \times 10^{-13}$ cm^3 $molecule^{-1}$ s^{-1} as an estimate for the rate constant. Future work is planned to study reaction 9 by independently adding HF to the reactor and observing the decay of NF(a). At that time the role of (8) vs. (9) can be ascertained. Heidner and co-workers[21] give even a smaller limit, $\leq 1 \times 10^{-13}$ cm^3 $molecule^{-1}$ s^{-1}, for the self-destruction of NF(a), which suggests that HF quenching is important. The small value for k_8 is surprising in view of the NCl and NF self-destruction rate constants,[7,19,10a] which are reported as $\sim 10^{-11}$ cm^3 $molecule^{-1}$ s^{-1}. These reports presumably are for the ground-state self-destruction reaction rather than for the first singlet state. In any event, the value for k_8 must be less than 10^{-12} cm^3 $molecule^{-1}$ s^{-1} in order for the [NF(a)] shown in Figure 8 to be observable for 0.2 s.

Another observation from Figure 8 is the rather low [NF(a)] for experiments with $[F] \approx 2[HN_3]$. As the concentration of $[HN_3]$ was increased, it was difficult to maintain [F] in excess by factors of 5–8, as done for experiments shown in Figure 5. One explanation is that although the N_3 concentration was larger, the [F] was insufficient to rapidly convert the [N_3] to [NF(a)]; hence, the N_3 bimolecular self-destruction reaction became important.

$$2N_3 \rightarrow 3N_2 \qquad \Delta H^\circ_0 = -227 \text{ kcal mol}^{-1} \quad (10)$$

Fitting data of Figure 8 and other similar experiments using the previously determined value for k_4 suggested $k_{10} \approx 2^{+2}_{-1} \times 10^{-11}$ cm^3 $molecule^{-1}$ s^{-1}. The value of k_{10} affects the maximum yield of NF(a) for $[F] \gtrsim 2[HN_3]$ conditions and this was the main

(18) Pritt, Jr., A. T.; Patel, D.; Coombe, R. D. *J. Chem. Phys.* **1981**, *75*, 5720.

(19) Clyne, M. A. A.; MacRobert, A. J. *J. Chem. Soc., Faraday Trans. 2* **1983**, *79*, 283. **1985**, *81*, 159.

(20) Jourdain, J. L.; LeBras, G.; Poulet, G.; Combourieu, J. *Combust. Flame* **1979**, *34*, 13.

(21) Koffend, J. B.; Gardner, C. E.; Heidner, III, R. F. *J. Chem. Phys.* **1985**, *83*, 2904.

experimental observation used in assigning k_{10}. Since our assignment depends on both k_4 and [F], the value for k_{10} has considerable uncertainty. Jourdain and co-workers[20] estimated k_{10} as 7×10^{-11} cm^3 molecule^{-1} s^{-1} from measurements in the ClN_3 system. However, we believe that k_{10} must be less than k_4.

The Secondary Reaction: Observations in an Uncoated Reactor. Most published studies[1,2,22] of the F + HN_3 reaction find strong $N_2(B^3\Pi_g-A^3\Sigma_u^+)$ emission and, at least, imply that the [NF(a)] may be substantially less than the starting NH_3. Since we never observed any N_2(B–A) emission in our halocarbon-coated reactor and since our value of k_4 was larger that the previous estimate,[2a] we did some experiments in an uncoated 7-cm-diameter Pyrex glass reactor for [HN_3] = (1–2) $\times 10^{12}$ molecule cm^{-3} for variable [F]. We observed that the N_2(B–A) emission intensity was strong relative to the NF(a–X) emission intensity. The N_2(B) vibrational distribution was similar to that found by David and Coombe.[22] In addition, we observed the NH(A–X) emission band in the ultraviolet from N_2(A) + HN_3. Since N_2(B–A) emission was *not* observed in the halocarbon-coated reactor for the same [HN_3], reaction 10 is not responsible for the observed N_2(B) formation and the following mechanism is proposed.[22]

$$N_3 + \text{surface} \rightarrow N_2 + N(^4S) \qquad \Delta H°_0 = 1 \text{ kcal mol}^{-1} \quad (11)$$

$$N(^4S) + N_3 \rightarrow N_2(B) + N_2(X) \qquad \Delta H°_0 = -55 \text{ kcal mol}^{-1} \quad (12)$$

Reactions 11 and 12 introduce N_2(A), N, and NH (from N_2(A) + HN_3) into the system and the kinetics can become extremely complex, especially at high concentrations. The N_2(B–A) intensity decreased and the NF(a–X) intensity increased as the [F]/[HN_3] ratio was increased. After these qualitative experiments were completed, this new reactor was coated with halocarbon wax and the F + HN_3 reaction was reinvestigated. New data were collected which confirmed the kinetics displayed in Figures 5 and 8; furthermore, the N_2(B–A) emission was absent in the coated reactor.

Discussion

The F + HN_3 Primary Reaction. The nascent HF(v) distribution is P_1–P_4 = 36:36:22:06. If $P_0 \approx P_1$, the HF($v \geq 0$) formation rate constant is $(1.1 \pm 0.2) \times 10^{-10}$ cm^3 molecule^{-1} s^{-1}. There was no evidence for a significant secondary reaction giving HF(v), and the infrared emission is consistent with HF(v) formation by a very fast primary reaction. Considering the availability of only one H atom per HN_3 molecule, reaction 1 has a very large rate constant. The D_0(H–N_3) was estimated as $\leq$93.4 kcal mol^{-1} based upon the highest observed HF(v,J) levels for v = 2, 3, and 4; this corresponds to $\Delta H_f°_0(N_3) \geq 113.6$ kal mol^{-1}, based upon $\Delta H_f°_0$(H–N_3)[23] = 71.8 kcal mol^{-1}. This value is approximately 10 kcal mol^{-1} higher than the value reported in standard data tabulations;[24] Clark and Clyne[25] favored $\Delta H_f°_0(N_3)$ = 99 kcal mol^{-1} based upon the highest observed product energies in the O and N atom reactions with N_3. A larger $\Delta H_f°_0(N_3)$ increases the available energy, and $\Delta H_f°_{30}(N_3)$ = 113.6 kcal mol^{-1} does not conflict with their measured product energies, i.e., the Clark and Clyne measurements are lower limits to $\Delta H_f°_0(N_3)$. An interesting consequence of $\Delta H_f°_0(N_3)$ = 113.6 kcal mol^{-1} is D_0(N_2–N) $\approx$ 1 kcal mol^{-1} for dissociation to N(^{4}S), and only the potential energy barrier arising from the surface crossing for dissociation to N(^{4}S) vs. N(^{2}D) renders N_3 a stable radical at room temperature. An interesting consequence of the revised $\Delta H_f°_0(N_3)$ is that reaction 12 provides essentially the same energy as N atom recombination.

The vibrational distribution and the highest HF(v,J) level measured in our fast flow reactor differs from the cold-wall arrested relaxation observations; see Table I. There are several F atom reaction systems which have discrepancies in the HF(v) distributions measured by the two techniques.[8b] One possible explanation in the present case is the purity of the HN_3. Water contamination in the HN_3 preparation could partly explain the lower HF(v) distribution found by Sloan and Watson.[1] The weak emission from HF(v=5) for high [F] and [HN_3] is another important discrepancy.[1] In accord with the old D_0(H–N_3), they associated HF(v=5) formation with direct abstraction and the majority of the HF(v=1–4) formation to reaction 3. Other investigators[2] also have mentioned observation of HF(v=5) from overtone spectra for high concentration conditions; however, we never observed HF(v=5) from our experiments. We suggest that HF(v=5) could be formed by an energy-pooling secondary reaction, perhaps HF(v=2 or 3) + NF(a), especially at higher concentrations (flows). Since our highest observed HF(v,J) states give a D_0(H–N_3) value in agreement with the proton affinity measurements[16] of N_3^-, we conclude HF(v=5) is not a primary product from reaction 1. Another possible explanation for HF(v=5) formation could be a minor reaction channel giving N_2 + HNF followed by F + HNF to form HF(v) + HF(X). This possibility was favored by Dyke et al.[26] who used F + HN_3 to generate N_3 for photoelectron spectroscopy measurements. Our data would not exclude 10% of the reaction proceeding by this route.

Formation of HF and N_3 can take place by two mechanisms: direct abstraction of H atom over a repulsive potential surface (reaction 1) and formation of an activated FHN_3* complex, which subsequently eliminates HF(v) (reaction 2). The fact that the HF(v,J) distributions extend to the thermochemical limit for each HF(v) level does not formally eliminate reaction 3 because D_0(N_2–N) is approximately zero. However, dynamical arguments coupled with the HF(v,J) distribution suggest that reation 3 is unlikely, because the N_2 product, in the first step, and translational motion, in the second step, probably would retain considerable energy. Furthermore, the favored N atom state from HF elimination from HNF* would not be the ground N(^{4}S) state. An even more compelling argument is that reaction 3 provides no pathway for NF(a) formation in a secondary reaction. Thus, the discussion for the primary reaction pathway can be focused upon reactions 1 and 2. This conclusion is reinforced by photoelectron spectroscopic observations of N_3 from the F + HN_3 system.[26]

In general, unimolecular HF elimination reactions favor noninverted vibrational distributions[8,27] and low $\langle f_V(HF) \rangle$, whereas direct H atom abstraction reactions by F atoms normally give inverted distributions[8] with $\langle f_V(HF) \rangle \approx 0.5$. Although the HF($v$) distribution for F + HN_3 is rather flat and $\langle f_V(HF) \rangle$ = 0.37–0.43 is lower than for many H-atom abstraction reactions, the HF(v) distribution still seems consistent with H abstraction, with perhaps some contribution from the addition channel. In particular, the HF(v) distribution resembles that from F + H_2S or F + NH_3 reactions.[8,28] The high J envelopes of the steady-state HF(v) rotational distributions also are consistent with HF rotational distributions from abstraction reactions of similar $\langle E \rangle$.[8]

The vibrational energy retained by N_3 is an important question since previous investigators[2] have suggested that N_3 from (1) is partly dissociated. The activation energy for N_3 decomposition is not known so this cannot be used to set a limit upon $\langle E_V(N_3) \rangle$. Except for reactions yielding radicals with large stabilization energies, H abstraction reactions do not release significant amounts of vibrational energy to the radical product.[8] The N–N bond lengths change from 1.237 and 1.133 Å in HN_3[29] to 1.18 Å[26] and N_3 may acquire some vibrational energy as a consequence of these

(22) (a) David, S. J.; Coombe, R. D. *J. Phys. Chem.* **1985**, *89*, 5206. (b) David, S. J.; Coombe, R. D. *J. Phys. Chem.* **1986**, *90*, 3260.
(23) Evans, B. L.; Gray, P.; Yoffe, A. D. *Chem. Rev.* **1959**, *59*, 515.
(24) Stull, D. R.; Prophet, H. *Natl. Stand. Ref. Data Ser., Natl. Bur. Stand.* **1971**, *No. 34*.
(25) Clark, T. C.; Clyne, M. A. A. *Trans. Faraday Soc.* **1970**, *66*, 877.
(26) (a) Dyke, J. M.; Jonathan, N. B. H.; Lewis, A. E.; Morris, A. *Mol. Phys.* **1982**, *47*, 1231. (b) Ab initio calculations[26a] find a slightly lower (604 cm^{-1}) energy for a $C_{\infty v}$ geometry than for a $D_{\infty h}$ geometry with the calculated N_3(X) bond lengths of 1.227 and 1.135 Å. However, the authors conclude in favor of a $D_{\infty h}$ structure.
(27) (a) Zamir, E.; Levine, R. D. *Chem. Phys.* **1980**, *52*, 253. (b) Donaldson, D. J.; Watson, D. G.; Sloan, J. J. *Chem. Phys.* **1982**, *68*, 95.
(28) (a) Wategaonkar, S.; Setser, D. W. *J. Chem. Phys.*, submitted for publication. (b) Donaldson, D. J.; Parsons, J.; Sloan, J. J; Stolow, A. *Chem. Phys.* **1984**, *85*, 47.
(29) (a) Herzberg, G. *Molecular Spectra and Molecular Structure III*; Van Nostrand: New York, 1966. (b) Winnewisser, M.; Cook, R. L. *J. Chem. Phys.* **1964**, *41*, 999. (c) Harrison, S. W.; Fisher, C. R.; Kemmey, P. J. *Chem. Phys. Lett.* **1975**, *36*, 229.

bond length changes after the H atom has been transferred to F. However, no evidence was found in this work for gas-phase N_3 dissociation since $N_2(B^3\Pi_g-A^3\Sigma_u^+)$ emission from N + N_3 was not observed in experiments with the coated reactors, even for the high concentration measurements reported in Figure 8.

The F + N_3 Secondary Reaction. The thermochemistry used for reaction 4 was based upon $\Delta H_f°_0(N_3)$ = 113.6 kcal mol^{-1} and $\Delta H_f°_0(NF)$[24] = 59.5 kcal mol^{-1}. The latter value has received some support from ab initio calculations.[30] Our results show that formation of NF(a) is the main reaction channel from F + N_3 and we assign a rate constant of $(5 \pm 2) \times 10^{-11}$ cm^3 molecule^{-1} s^{-1}. Formation of NF(b) is 10^{-4} times smaller than for NF(a). The NF(X) yield is not well characterized, but can be no more than ~0.1 of the total NF product. The rate constant for reaction 4 is similar to the value[20] for Cl + N_3, $(1.0 \pm 0.4) \times 10^{-11}$ cm^3 molecule^{-1} s^{-1}. Using basically the same approach as employed in this study but higher [F] and [HN_3] and a teflon reactor, Pritt and co-workers[2a] assigned k_4 as 2×10^{-12} cm^3 molecule^{-1} s^{-1}. The slower rise time for [NF(a)] possibly was a consequence of poor mixing or complications associated with N, NH, and N_2(A, W, B) in the system. As [HN_3] is increased, care must be exercised to maintain excess [F] in order to avoid reaction 10 because of the large N_3 concentration. As the NF(a) concentration increases to the 10^{13} molecule cm^{-3} level, the self-destruction reaction (or quenching by HF) also must be considered.

The value for k_4 is important because the F atom reaction is used in competitive experiments to measure other rate constants,[22] for example k_{12}. Therefore, after this program of study was completed, additional data were acquired in a new reactor to check the fitting in Figure 5, as explained in the Results section. The general nature of the prior data were reproduced with regard to both the NF(a) emission intensity for a given [HN_3] and the time dependence of [NF(a)] formation vs. [F].

Since the F + HN_3 reaction is fast, reaction 1 also can be used as a chemical source for N_3 radicals, if [F] is controlled. The F + HN_3 reaction has recently been utilized to generate N_3 for study of the reaction between N and N_3[22] and several studies have been published concerning the reactions of Cl and Br with N_3.[2b,c,19] From the N_2(B) emission intensity from the reaction of N with N_3, David and Coombe derived a rate constant for F + HN_3 of $(1.6 \pm 0.2) \times 10^{-10}$ cm^3 molecule^{-1} s^{-1}, which is in agreement with our measurement. One aspect of our work which is not in agreement with David and Coombe's interpretation is the use of a small rate constant for k_4; we doubt that the reaction of F with N_3 can be neglected in analysis of the F/N/HN_3 system,[22] and this may explain the current discrepancy in the rate constant measurements for N + N_3.[22,31] The bimolecular self-destruction rate constant for N_3 is not well determined. Yamasaki et al.[31] reported 1.4×10^{-12} cm^3 molecule^{-1} s^{-1} for the component giving N_2(B), whereas Jourdain et al. favored $(5–8) \times 10^{-11}$ cm^3 molecule^{-1} s^{-1} for the total rate constant. The measurement by Yamasaki et al. is based on the residual N_2(B–A) intensity with no added N, in their Cl + HN_3 system. If there was some surface initiated decomposition of N_3, their measurement could be too high. If our estimate for k_4 is accepted, k_{10} must be in the range $\sim 2 \times 10^{-11}$ cm^3 molecule^{-1} s^{-1}.

The explanation for the product specificity of F + N_3 must depend, at least in part, upon the dissociation of the ground singlet FN_3 potential (^{1}A′), which correlates to N_2(X) + NF(a). The excited state $FN_3(^1A'')$ surface also correlates to NF(a) + N_2 and provides another pathway. The formation of only NF(a) in the $v' = 0$ level is somewhat surprising in view of the 40 kcal mol^{-1} of excess energy. This may be evidence for the importance of the more repulsive ^{1}A″ pathway, which would favor translational energy release. The large excess vibrational energy of the chemically activated $FN_3(^1A')$ molecules would lead to a short lifetime and the crossing with the triplet surface (^{3}A″) leading to N_2 + NF($X^3\Sigma^-$) would not be very effective. This behavior for the chemically activated $FN_3(^1A')$ molecule can be contrasted to the thermal dissociation[32] of HN_3 for which N_2 + NH($X^3\Sigma^-$) are thought to be the products for temperatures below ~1300 K. The singlet–triplet surface crossing for HN_3 is ~17 kcal mol^{-1} below the N_2 + NH($a^1\Delta$) dissociation limit and thermal activation favors dissociation via the lower energy pathway.[32,33] The states for NF and NH have similar energies and the crossing positions for the FN_3 and HN_3 potentials should be similar, even though $HN_3(^1A')$ is more strongly bound than $FN_3(^1A')$. Measurement of the product branching pathways for the H + N_3 reaction should be interesting.

The role of the triplet surfaces (^{3}A′,^{3}A″) and the other singlet surface originating from F + $N_3(^2\Pi_g)$ are not well understood; however, there must be a sufficient barrier in the entrance channel of the ^{3}A″ surface correlating to NF($X^3\Sigma^-$) + N_2 to preclude significant reaction on this triplet surface at room temperature. The situation is very similar to the other efficient reaction, eq 7, giving NF(a), which proceeds via the ground singlet surface to give chemically activated HNF_2, which unimolecularly eliminates HF to give NF(a). The reaction of Cl and Br with N_3 have been observed[1b,c,19,31a] to give NCl(a,b) and NBr(a,b). The a and b yields have not been established, but qualitative[1b] observations suggest that NCl(b) and NBr(b) are approximately 10% of the N_3 consumed. The b states are formed with a broad range of vibrational levels in contrast to the NF(a) state from the F + N_3 reaction. Since the energy of NCl(b) and NBr(b) are lower than for NF(b), possibly the second ^{1}A′ surface from Cl or Br + N_3 is responsible for NCl(b) or NBr(b) formation in competition with the two lower singlet pathways. Much remains to be learned about the potential surfaces arising from halogen atoms and N_3 radicals, but these reactions clearly are useful for generating excited-state products.

Conclusions

The F + HN_3 reaction system in a halocarbon wax coated flow reactor provides a chemical source for NF(a) molecues that complements the H + NF_2 reaction. The net NF(a) formation rates and the NF(a) yields for both systems are comparable; one requires excess F atoms and the other excess H atoms. There are fewer secondary reactions between F and NF(a) than between H and NF(a) and that can be advantageous for studies requiring long observation times. On the other hand, bimolecular self-destruction by N_3 radicals can be a disadvantage in the F/HN_3 system for experiments requiring high NF(a) concentrations. The choice for the NF(a) source largely depends upon the compatibility of the chemistry to be studied with the excess H or F atoms that are present. Estimates were made for the rate constants of the two principal interfering reactions, namely bimolecular self-destruction by $2N_3$ and 2NF(a) or NF(a) + HF. Qualitative observations suggest that collisions between N_3 and clean Pyrex glass surface induce dissociation to N and N_2. Subsequent fast reaction between N and N_3 introduces N_2(A, B, W) molecules into the system, which can cause complications. The primary reaction, F + HN_3, and the secondary reaction, F + N_3, were discussed at the state-to-state level. The primary reaction is judged to be largely an abstraction reaction. The F + N_3 step selects the singlet surfaces in preference to the triplet surfaces. Based upon the highest observed HF(v,J) level, revision of D_0(H–N_3) and $\Delta H_f°_0(N_3)$ are suggested.

Acknowledgment. This work was supported by the U.S. Air Force Weapons Laboratory and by the National Science Foundation (CHE-85-43609).

Registry No. F, 14762-94-8; HN_3, 7782-79-8; NF, 13967-06-1.

(30) Bettendorff, M.; Peyerimhoff, S. D. *Chem. Phys.* **1985**, *99*, 55.
(31) (a) Yamasaki, K.; Fueno, T.; Kajimoto, O. *Chem. Phys. Lett.* **1983**, *94*, 425. (b) Piper, L. G.; Krech, R. H.; Taylor, R. L. *J. Chem. Phys.* **1979**, *71*, 2099.
(32) Kajimoto, O.; Yamatoto, Y.; Fueno, T. *J. Phys. Chem.* **1979**, *83*, 429.
(33) Tokue, I.; Ito, Y. *Chem. Phys.* **1983**, *79*, 383.